Mickael Messaoudi*, Bruno Pouet
Sound & Bright, Los Angeles, USA

Recent development in all-optical ultrasonic shear wave inspection

Niedawne odkrycie w całkowicie optycznej ultradźwiękowej inspekcji fal poprzecznych

ABSTRACT

A laser-based technique for efficiently generating and detection ultrasonic shear-wave is described. For the detection, a new laser interferometric scheme was recently developed in order to measure the three components of the ultrasonic field. This scheme takes advantage of the large étendue achieved with interferometer based on two-wave mixing in photorefractive crystal. Detection of the out-of-plane component as well as the two orthogonal in-plane components of the surface displacement is achieved using a single laser probe beam and a single, large aperture, collecting optic combined with detector arrays. With this interferometer, all wave types can be detected. The detection of the in-plane component allows efficient detection of shear waves, particularly when the direction of ultrasounds propagation is normal to the surface of inspection. However, for remote shear wave inspection, one must also be able to efficiently generate normal incidence shear waves. With laser-based generation, shear waves are mainly generated off the normal incidence. In this paper, in addition to presenting the tri-component interferometer, an improved method for normal-incidence shear wave generation is described. The combination of shear-wave LU generation with a multi-component laser receiver makes LU pulse-echo shear-wave inspection possible. Results from characterization of the receiver and of the generation are shown.

Keywords: *laser ultrasound, in-plane displacement, three dimensional, directivity pattern, shear waves*

STRESZCZENIE

Opisano technikę laserową do wydajnego generowania i wykrywania ultradźwiękowych fal poprzecznych. W celu detekcji opracowano nowy laserowy układ interferometryczny do pomiaru trzech składników pola ultradźwiękowego. Schemat ten wykorzystuje dużą wartość uzyskaną przy pomocy interferometru opartego na mieszaniu dwóch fal w fotorefrakcyjnym krysztale. Wykrywanie elementu poza płaszczyzną, jak również dwóch ortogonalnych elementów w płaszczyźnie przemieszczenia powierzchni, uzyskuje się za pomocą pojedynczej wiązki sondy laserowej i pojedynczej, dużej apertury, zbierającej układ optyczny połączonej z układami detektorów. Za pomocą tego interferometru można wykryć wszystkie typy fal. Wykrywanie elementu w płaszczyźnie umożliwia skuteczne wykrywanie fal poprzecznych, szczególnie gdy kierunek propagacji ultradźwięków jest normalny do powierzchni kontroli. Jednak w przypadku zdalnej inspekcji fali poprzecznej ważne jest również by móc wydajnie generować padające fale poprzeczne. W przypadku generowania laserowego fale poprzeczne są wzbudzane głównie poza normalną . W niniejszej pracy, oprócz prezentacji interferometru trójskładnikowego, opisano ulepszoną metodę generowania padających fal normalnych. Połączenie generatora LU fali padającej z wieloskładnikowym odbiornikiem laserowym umożliwia inspekcję falą poprzeczną z wykorzystaniem trybu LU pulse-echo. Przedstawiono wyniki charakteryzacji odbiornika i generatora.

Słowa kluczowe: *ultradźwięki wzbudzane laserowo, przesunięcie w płaszczyźnie, trójwymiarowy, wzorzec kierunkowy, fale poprzeczne*

1. Introduction

Conventional laser-ultrasonic inspection is based on the detection of one component of the ultrasonic field, predominantly out-of-plane displacement of the inspected surface [1], [2]. A couple years ago, we developed a two wave mixing (TWM) interferometer capable of measuring two components of the surface displacement simultaneously, using a single laser probe [3]. Recently, our technology has been extended to develop a tri-component TWM interferometer, still relying on a single laser probe and with a 20 MHz detection bandwidth. The system simultaneously detects the out-of-plane, vertical and horizontal in-plane components of the surface displacement. Measurement of the in-plane component is very useful for the detection of shear waves. When generated with a laser, the far-field directivity pattern of the shear wave shows a zero at normal incidence, for generation in both the thermoelastic and ablation regimes. This weak shear-wave generation at normal incidence is due to the laser beam symmetry. Therefore, by altering the beam geometry, the amplitude of shear waves can be increased at normal incidence.

2. Tri-component interferometer

2.1 Principle

When ultrasounds reach the surface of inspection, they induce a small phase change of the backscattered laser beam. These small phase variations are converted into intensity variation after interference with reference beam in the two wave mixing (TWM) interferometer. We take advantage of the diffuse reflection, caused by the optical roughness of the surface when the incident receiver beam hits the sample, to collect the light backscattered at various angles, using a large collecting aperture. The large collection angle of scattered light is divided in elementary angles Θ_i which information contributes to the ultrasonic field reconstruction (Fig. 1). By imaging the collecting lens onto the detector we can separate each angular contribution. Each elementary angle carries phase information of both in-plane and out-of-plane contributions. The wider the angle is, the higher the in-plane sensitivity becomes.

The depth-of-field of the incident beam is very small due to the large collecting optic. To overcome this limitation, the collecting optic is mounted on a motorized translation, which can easily adjust the distance to the sample and compensate for variation in the sample flatness during scan. The light

*Corresponding author. E-mail: mickael.messaoudi@soundnbright.com

Published by „Badania Nieniszczące i Diagnostyka" SIMP Publishing Agenda
DOI: 10.26357/BNiD.2018.019

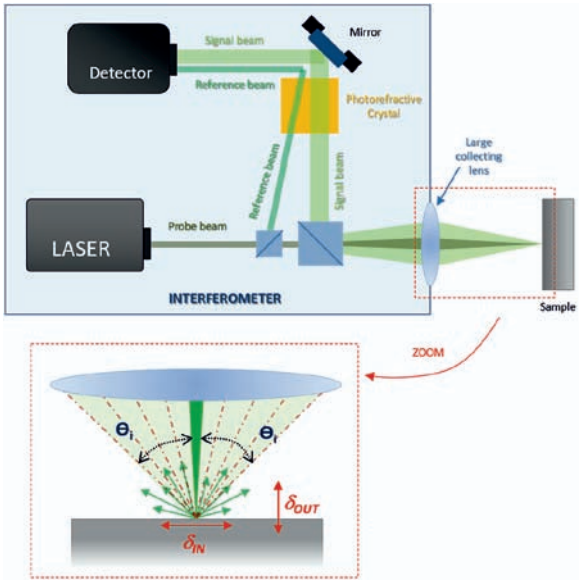

Fig. 1. Schematic of the interferometer with zoom on the reflection of single beam illumination on the sample.
Rys. 1. Schemat interferometru z powiększeniem odbicia pojedynczej wiązki na próbce.

collected by the front aperture is then separated into small angles, resulting in an N x N matrix of elements, each containing a fraction of the ultrasonic field information. A direct approach to data processing could be to decompose each of the N^2 elements but the large number of channels to process is challenging. Rather than using a N^2 matrix of photodiodes, the optical beam is divided in two: half of the collected light is focused on a vertical linear array of N elements using a vertical cylindrical lens, while the other half is focused on a horizontal linear array of N elements using a horizontal cylindrical lens. The vertical array provides information about the out-of-plane and the vertical in-plane, the horizontal array provides information about the out-of-plane and the horizontal in-plane, reducing the number of processed channels from N^2 to 2N. Each array is composed of 16 elements. Each element of the detector array corresponds to a small area of the entrance pupil and thus corresponds to light backscattered along well defined incidence angles (Fig. 2).

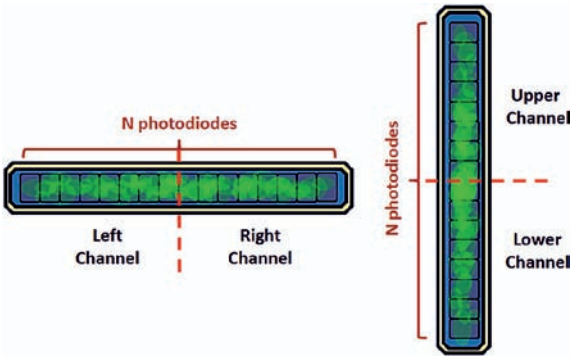

Fig. 2. Matrix N x N vs 2 linear arrays N + N.
Rys. 2. Macierz N x N vs 2 liniowe tablice N + N.

The light backscattered by the sample may not be uniformly distributed, therefore each channel must be normalized prior to calculating the two in-plane and the out-of-plane components of the surface displacement. Normalization is achieved by introducing a small, low-frequency phase change in the reference beam and using automatic gain controlled (AGC) amplifiers which monitor the low frequency signal and normalize each channels (Fig. 3). For each linear array, after amplitude normalization, the signals are processed in pairs of the same incidence angle. For each pair, the two normalized signals are added to each other in order to obtain the elementary out-of-plane component, while their subtraction yields the elementary in-plane component.

However, the contribution in the final in-plane signal of each elementary in-plane component depends on the angle. A weight is thus applied depending on the angle contribution of the in-plane as show equation (1) for the elementary in-plane and in equation (2) for the out-of-plane components.

$$I_i - I_{-i} \propto \left(\frac{4\pi\delta_{IN}}{\lambda}\right)\sin(q_i) \tag{1}$$

$$I_i + I_{-i} \propto \left(\frac{4\pi\delta_{OUT}}{\lambda}\right)\cos(q_i) \tag{2}$$

Ii is the intensity on one photodetector corresponding to the angle q_i of detection and I_{-i} its symmetric. δ_{IN} and δ_{OUT} are respectively the in-plane and out-of-plane displacement.

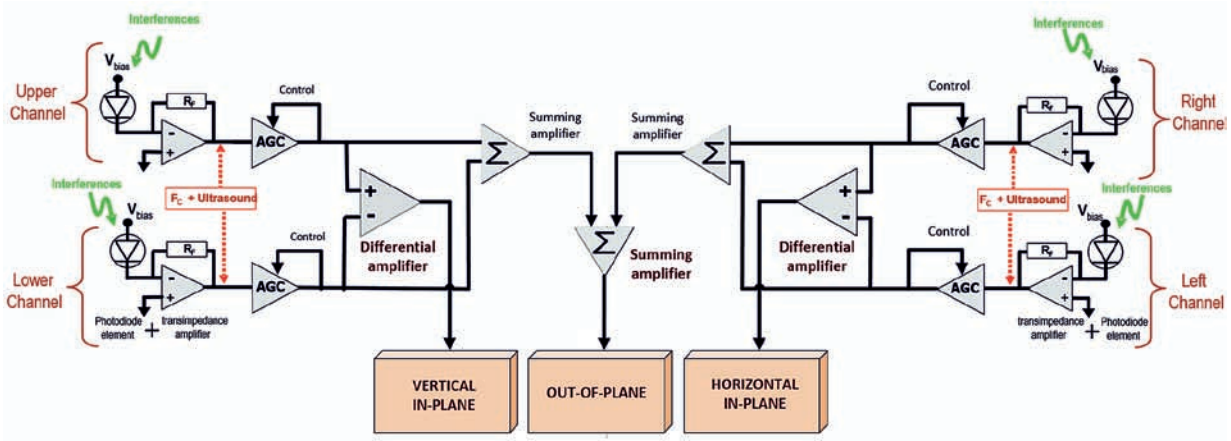

Fig. 3. Principle of the electronic demodulation circuitry.
Rys. 3. Zasada elektronicznego obwodu demodulacyjnego.

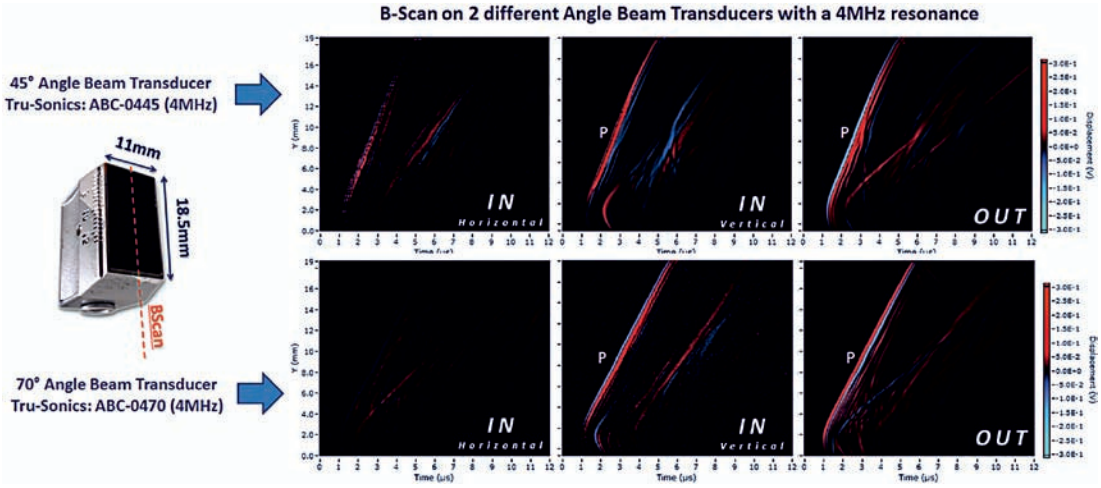

Fig. 4. B-scan results for Horizontal In-plane, Vertical In-plane and Out-of-plane measurement.
Rys. 4. B-skan dla pomiarów poziomych w płaszczyźnie, pionowych w płaszczyźnie i poza płaszczyzną.

2.2 Experimental results

Measurements were carried out using a 45° and a 70° angle beam transducers (Tru-sonics: ABC-0445 (4MHz) and Tru-sonics: ABC-0470 (4MHz)), generating compressional waves with an angle relative to the surface of inspection. In both cases, the surface was scanned along an 18.5 mm line across the transducer. The B-scan results for the three component contributions are shown in Fig. 4.

The measurements for each component were carried out with a calibration coefficient of 100mV/nm. Due to transducer geometry, the system should not detect any signal from the horizontal in-plane component. However, a very small signal is visible, probably due to the leakage of the strong out-of-plane component. A strong compressional wave is clearly visible in the vertical In-plane and Out-of-plane B-scans. Many reflected and converted wave arrivals are also visible.

3. Thermoelastic generation of shear waves

3.1 Principle

In the thermoelastic regime, the rapid absorption of the laser beam leads to a strong thermal gradient at the edge of the laser beam spot [4]. For a metal sample with a free surface, the thermal gradient induces stress which direction is parallel to the surface. Because of the source symmetry, the thermal expansion leads to a bipolar stress field (Fig. 5.a). If the symmetry of the beam is broken, the thermal expansion leads to a quasi-unipolar stress field (Fig. 5.b). In this case, the directivity of S-waves is changed and the amplitude increases at epicenter. Fig. 5c shows a simple arrangement for generating a dissymmetric thermal gradient with a very sharp edge on one side and a quasi-smooth edge on the other. The generation laser (pulsed Nd:YAG, λ = 1.064 nm) used for the demonstration is highly-multimode and includes some hot spots. Because of the not very smooth beam profile, the generation spot (Fig. 5c) still induces a strong temperature gradient of the curved tail edge, acting as a secondary (parasitic) ultrasonic source. The ultrasonic "ghost" signal due to the curved tail edge contribution can be easily separated from the signal of interest because of its different arrival time. It must be noted that a Gaussian beam intensity profile would be preferred as it would generate a smoother beam profile, reducing the "ghost" generation.

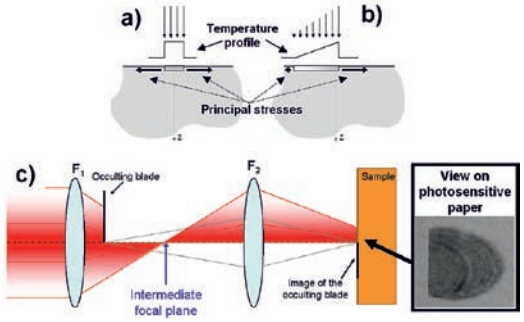

Fig. 5. Acoustic source formed by: A - a symmetrical illumination (bipolar) and B - an asymmetrical illumination (Unipolar); and C - Setup used for generating asymmetrical illumination.
Rys. 5. Źródło akustyczne utworzone przez: A - symetryczne oświetlenie (bipolarne) i B - asymetryczne oświetlenie (Unipolarne); i C - Konfiguracja używana do generowania asymetrycznego oświetlenia.

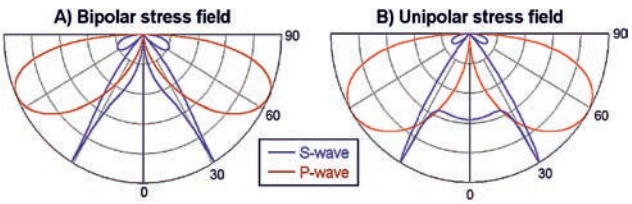

Fig. 6. Directivity for S-wave and P-wave calculated assuming: A - Bipolar stress field; B – Unipolar stress field.
Rys. 6. Kierunkowość dla fali S i P obliczona przy założeniu: A - bipolarnego pola naprężeń; B - jednobiegunowego pola naprężeń.

Fig. 6 shows the directivity patterns of P-waves and S-waves calculated using a half-cylinder of aluminum for a bipolar stress and for a unipolar stress [5]. The P-wave radiation patterns are very similar, with maximum around 60° incidence for both sources, the bipolar source being a little more directive. For both sources, the S-wave radiation patterns are at maximum near 30° incidence. As expected, the main difference is at normal incidence, where the unipolar source generates a strong S-wave and the bipolar source generates no S-wave.

3.2 Ultrasonic bulk waveforms in plates

Through-transmission measurements are carried out on an aluminum plate, 7.9 mm thick. The three orthogonal components of the surface displacement, the horizontal in-plane, the vertical in-plane and the out-of-plane were recorded over a [1MHz to 20 MHz] bandwidth (Fig. 7).

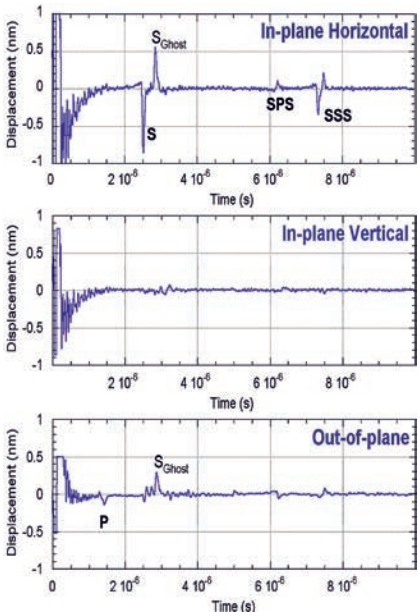

Fig. 7. The three components of the surface displacement generated by the asymmetrical source and measured at the epicenter (centered on the sharp edge).
Rys. 7. Trzy składowe przemieszczenia powierzchni generowane przez źródło asymetryczne i mierzone w epicentrum (wyśrodkowane na ostrych krawędziach).

As expected, we see a strong in-plane displacement corresponding to the on-axis S - wave arrivals. We used the following notation: S - direct transmitted S-wave, P - direct transmitted P-wave, SSS - 1st reflected S-wave (3 thicknesses) and SPS - converted wave. The in-plane displacement is mostly in the horizontal plane due to the symmetry of the source. The S-wave generated by the unipolar source corresponds to the sharp negative pulse (arriving at 2.5 μs). The smaller and not as sharp positive pulse arriving later (at 2.85 μs) corresponds to the parasitic effect from the curved tail edge. The amplitude of the P-wave is also very weak at the epicenter, as expected with thermoelastic generation.

Recording only the horizontal in-plane component, we carry out two B-scans by moving the detection along a line centered on the epicenter of the source (Fig. 8). The first B-scan shows the result obtained for a bipolar source by the horizontal in-plane component whereas the second one shows the result obtained for a unipolar source by the horizontal in-plane. Black color corresponds to negative displacement and white color corresponds to positive displacement. E -> indicates the position at epicenter. EG -> indicates the position centered on the curved tail edge, responsible for the "ghosts". The results are well in agreement with the bipolar and unipolar assumptions. For the unipolar source, the in-plane displacement direction does not change with the sign of the incidence angle. At the opposite, for the bipolar source, the in-plane displacement direction depends on the sign of the incidence angle and cancels out at the epicenter. The ghost arrivals for the unipolar source, due to curved tail edge, are clearly visible.

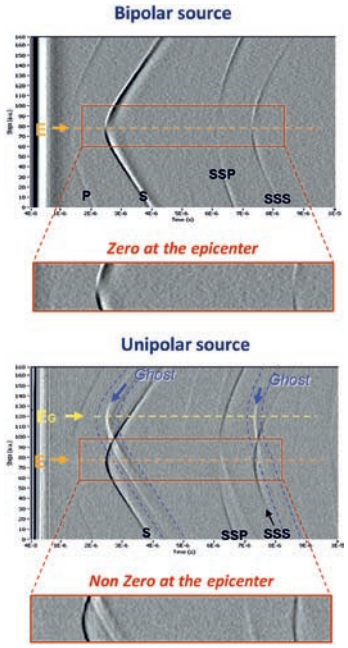

Fig. 8. Horizontal In-plane B-scans for a bipolar source and for a unipolar source after transmission through a 7.9 mm thick aluminum plate.
Rys. 8. B-skany w płaszczyźnie poziomej dla źródła dwubiegunowego i źródła unipolarnego po przejściu przez płytę aluminiową o grubości 7,9 mm.

4. Conclusions

The TEMPO 3D system was proven capable of measuring three components simultaneously using a single laser probe and a single collecting optic, providing data on the ultrasonic field. We have also presented an optical arrangement for improved thermoelastic generation of shear-waves, generating strong shear waves in the direction normal to the sample surface and opening up many possibilities for remote shear-wave inspection.

5. References/Literatura

[1] R.J. Dewhurst, Q. Shan, 'Optical remote measurement of ultrasound', Meas. Sci.Tech., 10 (11), pp.R139-R168, 1999.
[2] Monchalin, J.-P., Optical detection of ultrasound, IEEE Transactions on Ultrasonics, Ferroelectrics, and Frequency Control (ISSN 0885-3010), vol. UFFC-33, Sept. 1986, p. 485-499
[3] A. Wartelle et al., "Non-destructive testing using two component/two wave mixing interferometer", AIP Conference Proceedings. Eds. Donald O. Thompson, and Dale E. Chimenti. Vol. 1335. No. 1. AIP, 2011.
[4] B. Pouet, N. Lefaudeux, P. Clemenceau, S. Breugnot, "Laser Ultrasonic Inspection Based on In-Plane Detection and Shear Wave Generation", 1st International Symposium on Laser Ultrasonics: Science, Technology and Applications. July 16-18 2008, Montreal, Canada
[5] G.F. Miller and H. Pursey, 'the field and radiation impedance of mechanical radiators on a free surface of a semi-infinite isotropic solid', Proc. R. Soc. London, Ser. A 223, pp 521-541, 1954.